

Development and Comparative Analysis of Load Flow Algorithms on the IEEE 9-Bus Test System

Oshadha Samarakoon
 Registration No: E/21/345
 Course: EE354 Electric Power

Abstract

This report documents the implementation of a full Newton-Raphson load-flow solver for the IEEE 9-bus system, followed by method-level comparison with PSSE and voltage sensitivity analysis under independent load variations. All derivations, simulation logic, and result discussions are presented in technical form with reproducible tables and figure placeholders linked to the code workflow. The complete source code for this project is available at <https://github.com/Oshadha345/Electrical-Power/tree/main/EE354-Electric%20Power/Project>.

CONTENTS

I	Task 1: Program Development	2
I-A	Objective	2
I-B	Input Data Approach	2
I-C	Mathematical Formulation	2
I-D	Program Flowcharts with Line References	3
I-E	Y-bus Matrix from Code	4
I-F	Convergence and Sample Iteration Output	5
I-G	Execution Proof Requirement	5
I-H	Task 1 Discussion	6
II	Task 2: Verification and Comparison	7
II-A	Scope of Verification	7
II-B	Custom Program Recorded Outputs	7
II-C	Bus Voltage and Angle Comparison	7
II-D	Convergence Characteristics	7
II-E	Task 2 Plots	8
II-F	Discussion of Deviations	9
III	Task 3: Voltage Sensitivity Analysis	10
III-A	Method	10
III-B	Voltage Results Under Each Load Variation	10
III-C	Variance and Standard Deviation Tables	11
III-D	Task 3 Figures	12
III-E	Discussion of Findings	12
References		14

I. TASK 1: PROGRAM DEVELOPMENT

A. Objective

The objective of Task 1 is to develop a full Newton-Raphson load-flow program from first principles for the IEEE 9-bus system. The final code file is `E21345_LoadFlow.py`, which reads input from `IEEE9_Bus_system_data.json`, constructs the network admittance matrix in code, performs iterative NR solution, and reports voltages, mismatches, line flows, and system losses.

B. Input Data Approach

Power-flow programs can read data from several sources such as inline/manual input, text files, CSV files, or JSON files. In this work, JSON was selected because it provides structured key-value storage for buses, generators, transformers, lines, and loads in a readable format. The code still follows the assignment requirement of directly accepting text-file-based input.

TABLE I: Input dataset summary (from `IEEE9_Bus_system_data.json`).

Data block	Count
Buses	9
Generators	3
Transformers	3
Transmission lines	6
Load buses	3
Base power	100 MVA

C. Mathematical Formulation

The polar-form power-flow equations are solved using Newton-Raphson [1], [2], [3]:

$$P_i = \sum_{k=1}^n |V_i||V_k| (G_{ik} \cos \theta_{ik} + B_{ik} \sin \theta_{ik}), \quad (1)$$

$$Q_i = \sum_{k=1}^n |V_i||V_k| (G_{ik} \sin \theta_{ik} - B_{ik} \cos \theta_{ik}). \quad (2)$$

The mismatch vector and update are:

$$\Delta \mathbf{f} = \begin{bmatrix} \Delta \mathbf{P} \\ \Delta \mathbf{Q} \end{bmatrix}, \quad \mathbf{J} \Delta \mathbf{x} = \Delta \mathbf{f}, \quad \mathbf{x}^{(k+1)} = \mathbf{x}^{(k)} + \Delta \mathbf{x}, \quad (3)$$

with Jacobian partition

$$\mathbf{J} = \begin{bmatrix} J_1 & J_2 \\ J_3 & J_4 \end{bmatrix}. \quad (4)$$

Model settings used in code:

- Slack bus: 1
- PV buses: 2, 3
- PQ buses: 4, 5, 6, 7, 8, 9
- Flat start: all unknown $|V| = 1.0$ p.u., all angles = 0°
- Convergence tolerance: 10^{-4} p.u. mismatch

D. Program Flowcharts with Line References

Following charts are the flow charts with line references. Figures 1, 2, and 3 are the exported flowcharts corresponding to the final script.

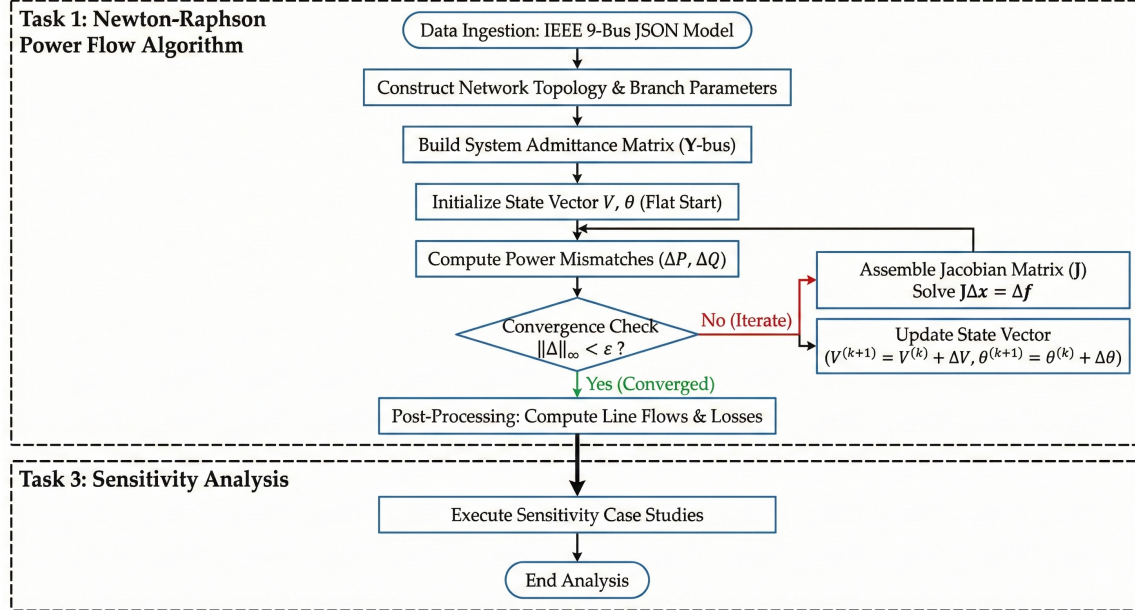


Fig. 1: Overall project workflow used to organize Tasks 1–3.

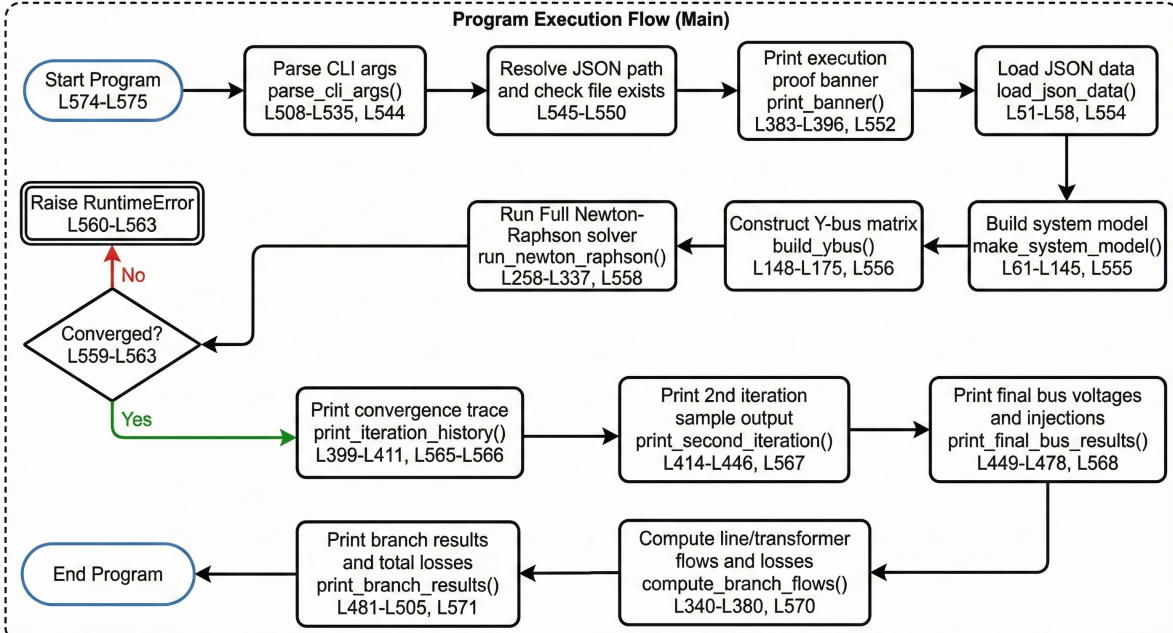


Fig. 2: Task 1 source-code flowchart linked to `E21345_LoadFlow.py` line ranges.

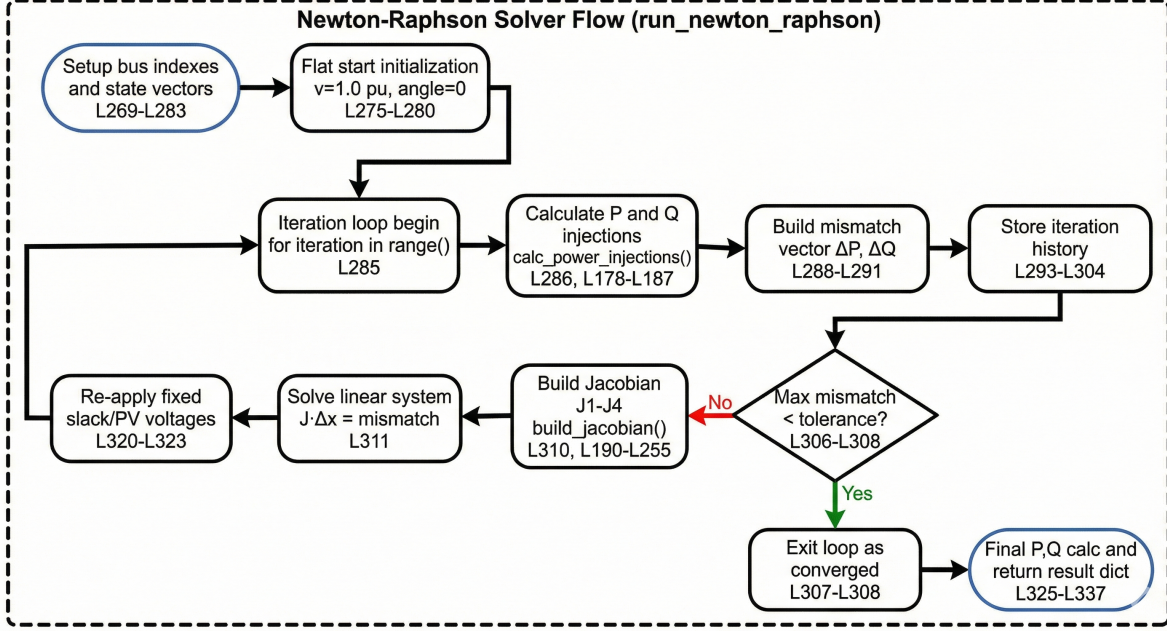


Fig. 3: Newton-Raphson internal function flowchart (mismatch, Jacobian, correction loop).

E. Y-bus Matrix from Code

The Y-bus matrix is built directly from line/transformer data in code (no hand calculation). The **real and imaginary parts** are shown in Tables II and III.

TABLE II: **Real** part of Y_{bus} (p.u.).

Bus	1	2	3	4	5	6	7	8	9
1	0.00000	0.00000	0.00000	0.00000	0.00000	0.00000	0.00000	0.00000	0.00000
2	0.00000	0.00000	0.00000	0.00000	0.00000	0.00000	0.00000	0.00000	0.00000
3	0.00000	0.00000	0.00000	0.00000	0.00000	0.00000	0.00000	0.00000	0.00000
4	0.00000	0.00000	0.00000	3.30738	-1.36519	-1.94219	0.00000	0.00000	0.00000
5	0.00000	0.00000	0.00000	-1.36519	2.55279	0.00000	-1.18760	0.00000	0.00000
6	0.00000	0.00000	0.00000	-1.94219	0.00000	3.22420	0.00000	0.00000	-1.28201
7	0.00000	0.00000	0.00000	0.00000	-1.18760	0.00000	2.80473	-1.61712	0.00000
8	0.00000	0.00000	0.00000	0.00000	0.00000	0.00000	-1.61712	2.77221	-1.15509
9	0.00000	0.00000	0.00000	0.00000	0.00000	-1.28201	0.00000	-1.15509	2.43710

TABLE III: **Imaginary** part of Y_{bus} (p.u.).

Bus	1	2	3	4	5	6	7	8	9
1	-17.36111	0.00000	0.00000	17.36111	0.00000	0.00000	0.00000	0.00000	0.00000
2	0.00000	-16.00000	0.00000	0.00000	0.00000	0.00000	16.00000	0.00000	0.00000
3	0.00000	0.00000	-17.06485	0.00000	0.00000	0.00000	0.00000	0.00000	17.06485
4	17.36111	0.00000	0.00000	-39.30889	11.60410	10.51068	0.00000	0.00000	0.00000
5	0.00000	0.00000	0.00000	11.60410	-17.33823	0.00000	5.97513	0.00000	0.00000
6	0.00000	0.00000	0.00000	10.51068	0.00000	-15.84093	0.00000	0.00000	5.58824
7	0.00000	16.00000	0.00000	0.00000	5.97513	0.00000	-35.44561	13.69798	0.00000
8	0.00000	0.00000	0.00000	0.00000	0.00000	0.00000	13.69798	-23.30325	9.78427
9	0.00000	0.00000	17.06485	0.00000	0.00000	5.58824	0.00000	9.78427	-32.15386

F. Convergence and Sample Iteration Output

TABLE IV: Task 1 convergence summary for IEEE 9-bus base case.

Item	Value
Tolerance	10^{-4} p.u.
Total iterations to convergence	4
Total active power loss	4.641023 MW
Total reactive power loss	-92.160126 MVAr

TABLE V: Second-iteration bus snapshot.

Bus	$ V _{iter2}$ (p.u.)	θ_{iter2} (deg)	P_{calc} (p.u.)	Q_{calc} (p.u.)
1	1.040000	0.000000	0.692229	0.131738
2	1.025000	9.891070	1.687927	-0.116864
3	1.025000	5.199844	0.883627	-0.240382
4	1.033415	-2.126114	0.010614	0.050091
5	1.008445	-3.828628	-1.287904	-0.428586
6	1.022349	-3.595802	-0.943938	-0.257555
7	1.037245	4.196429	0.042054	0.187516
8	1.026641	1.093843	-1.061005	-0.325875
9	1.039970	2.415549	0.026887	0.082844

TABLE VI: Final bus profile from custom NR solver.

Bus	$ V $ (p.u.)	Angle (deg)	$P_{injection}$ (MW)	$Q_{injection}$ (MVAr)
1	1.040000	0.000000	71.641012	27.045892
2	1.025000	9.280008	163.000003	6.653621
3	1.025000	4.664753	85.000001	-10.859733
4	1.025788	-2.216787	-0.000008	0.000006
5	0.995631	-3.988804	-125.000009	-49.999972
6	1.012654	-3.687395	-90.000008	-29.999988
7	1.025769	3.719704	0.000034	0.000033
8	1.015883	0.727538	-100.000018	-34.999992
9	1.032353	1.966718	0.000016	0.000008

TABLE VII: Line/transformer power flows and branch losses from custom NR run.

Branch	$P_{i \rightarrow j}$ MW	$Q_{i \rightarrow j}$ MVAr	$P_{j \rightarrow i}$ MW	$Q_{j \rightarrow i}$ MVAr	P_{loss} MW	Q_{loss} MVAr
T(1-4)	71.6410	27.0459	-71.6410	-23.9231	0.0000	3.1228
T(2-7)	163.0000	6.6536	-163.0000	9.1782	0.0000	15.8318
T(3-9)	85.0000	-10.8597	-85.0000	14.9554	0.0000	4.0956
L(4-5)	40.9373	22.8931	-40.6798	-38.6872	0.2575	-15.7941
L(4-6)	30.7037	1.0300	-30.5373	-16.5434	0.1664	-15.5134
L(5-7)	-84.3202	-11.3127	86.6202	-8.3808	2.3000	-19.6936
L(6-9)	-59.4628	-13.4566	60.8166	-18.0748	1.3538	-31.5315
L(7-8)	76.3799	-0.7973	-75.9046	-10.7042	0.4753	-11.5015
L(8-9)	-24.0954	-24.2958	24.1834	3.1195	0.0880	-21.1763

G. Execution Proof Requirement

The source code prints student identification and timestamp at runtime. Executed outputs are as follows, with screenshots provided in Figure 4.

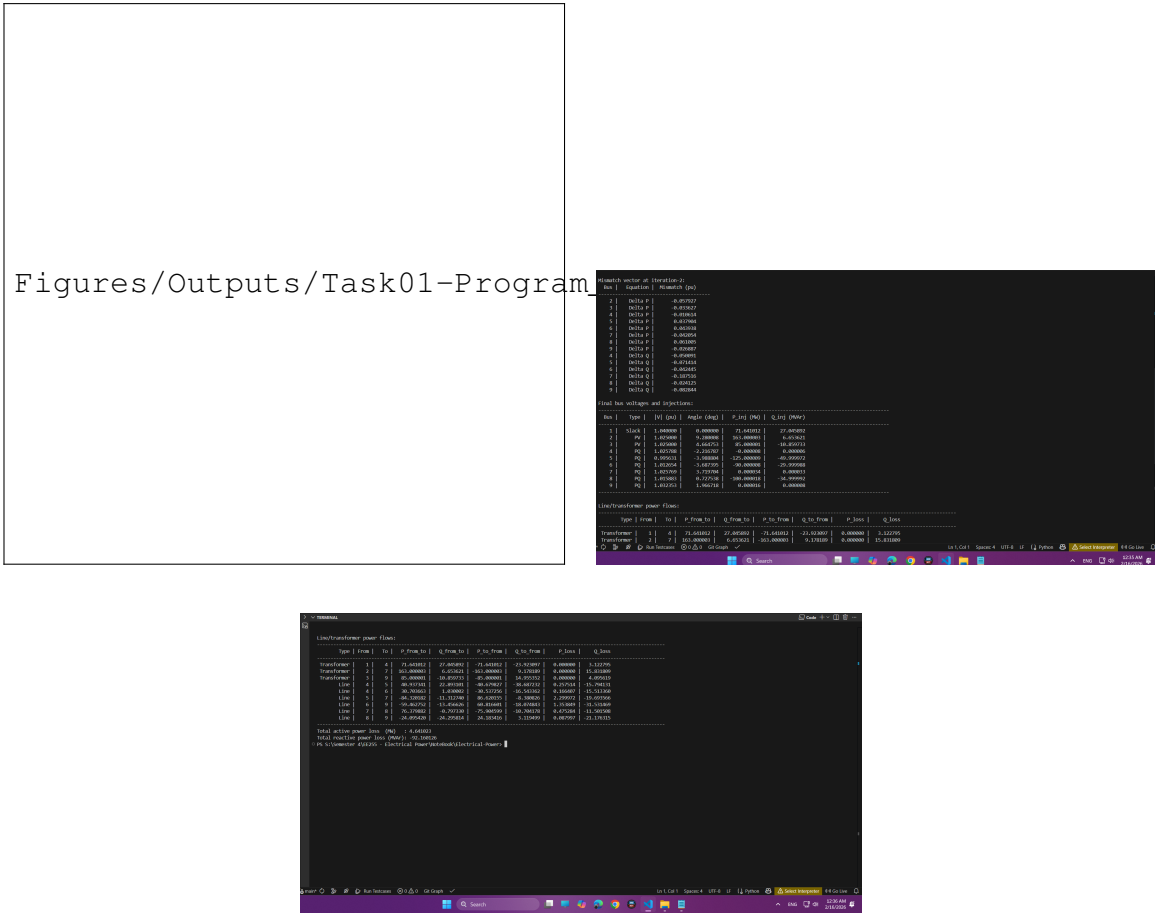


Fig. 4: Execution proof showing program output with student ID and timestamp.

H. Task 1 Discussion

The custom NR solver converged in four iterations with monotonic mismatch reduction. The solved operating point and branch-flow pattern are consistent with textbook IEEE 9-bus behavior and with expected NR convergence properties [1], [3], [4]. The transformer branches carry no active loss due zero resistance assumptions in the provided dataset, while transmission lines account for the net active losses. The obtained loss level (about 4.64 MW) is reasonable for this loading pattern and network parameters.

II. TASK 2: VERIFICATION AND COMPARISON

A. Scope of Verification

Task 2 verifies the custom NR program against PSSE outputs and compares:

- numerical accuracy in bus $|V|$ and angle,
- convergence behavior of NR, GS, and FDLF,
- likely reasons for observed differences.

PSSE data were taken from the uploaded solver logs [?] and bus report file [?].

B. Custom Program Recorded Outputs

From the custom Task-1 run:

- converged in 4 iterations at 10^{-4} p.u. tolerance,
- total loss $P_{loss} = 4.641023$ MW and $Q_{loss} = -92.160126$ MVAr,
- bus-voltage profile shown in Table VIII.

C. Bus Voltage and Angle Comparison

TABLE VIII: Bus-wise comparison between custom NR and PSSE bus report values.

Bus	Custom $ V $	PSSE $ V $	$ \Delta V $	$ \Delta V /\%$	Custom θ	PSSE θ
1	1.040000	1.0400	0.000000	0.000000	0.000000	0.0
2	1.025000	1.0250	0.000000	0.000000	9.280008	9.3
3	1.025000	1.0250	0.000000	0.000000	4.664753	4.7
4	1.025788	1.0258	0.000012	0.001130	-2.216787	-2.2
5	0.995631	0.9956	0.000031	0.003103	-3.988804	-4.0
6	1.012654	1.0127	0.000046	0.004508	-3.687395	-3.7
7	1.025769	1.0257	0.000069	0.006766	3.719704	3.7
8	1.015883	1.0159	0.000017	0.001712	0.727538	0.7
9	1.032353	1.0323	0.000053	0.005131	1.966718	2.0

TABLE IX: Numerical-accuracy summary (custom NR vs PSSE).

Metric	Value
MAE Voltage	0.000025 p.u.
RMSE Voltage	0.000035 p.u.
Max Voltage Error	0.000069 p.u.
MAE Angle	0.019594 deg
RMSE Angle	0.022267 deg
Max Angle Error	0.035247 deg

D. Convergence Characteristics

TABLE X: Convergence comparison using custom and PSSE solver outputs.

Method	Iterations	Largest mismatch (MVA)	System abs mismatch (MVA)	Stability
Custom NR	4	0.000034	–	Converged
PSSE NR	3	0.00	0.00	Converged
PSSE FDLF	3	0.02	0.04	Converged
PSSE GS	18	0.20	0.85	Converged (slow)

TABLE XI: Loss comparison (available from uploaded outputs).

Method	Total P_{loss} (MW)	Note
Custom NR	4.641023	From program branch-flow summation
PSSE bus report	4.6 (approx.)	From rounded branch MW values in uploaded report
PSSE GS / FDLF	–	<i>TODO: export method-specific branch report if strict per-method loss is required</i>

E. Task 2 Plots

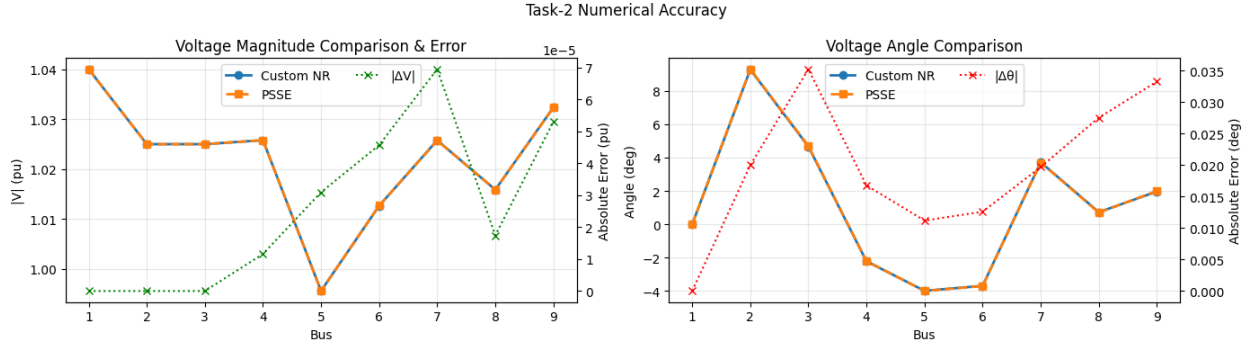


Fig. 5: Voltage magnitude and angle comparison plot (custom vs PSSE).

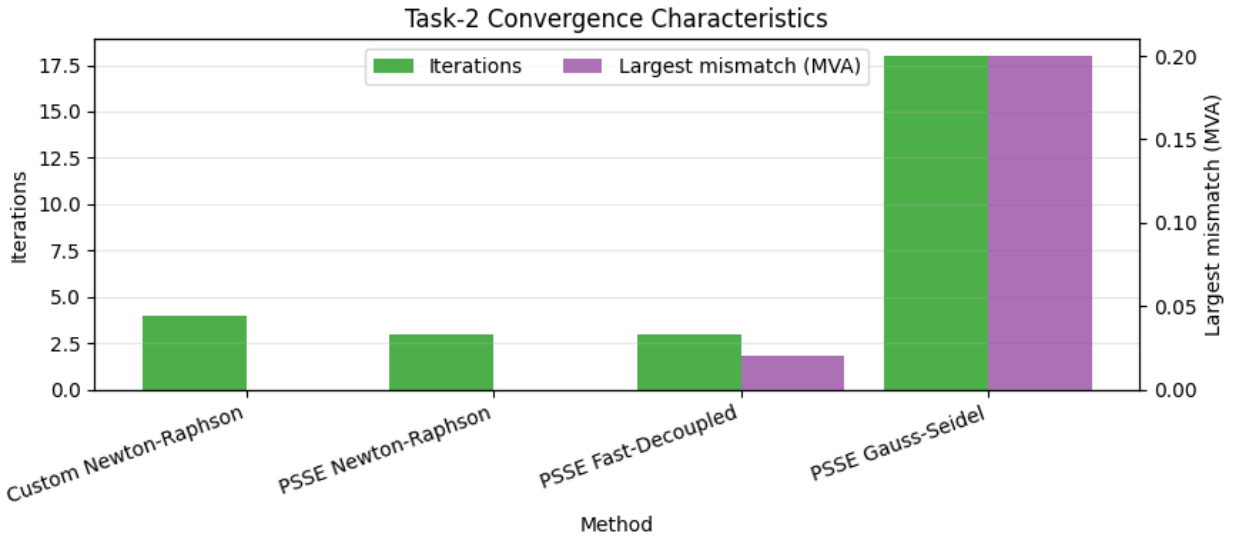


Fig. 6: Convergence characteristics: iteration count and mismatch level by method.

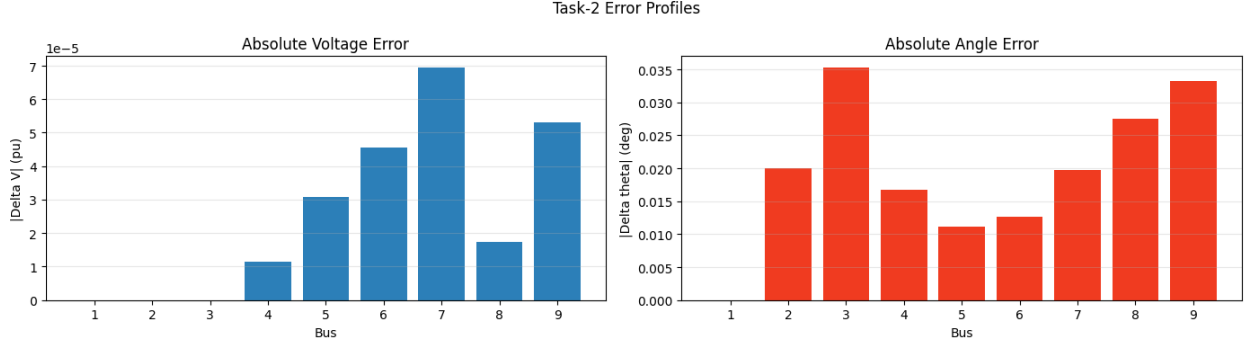


Fig. 7: Voltage and angle absolute error profiles across buses.

F. Discussion of Deviations

The bus-voltage differences between custom NR and PSSE are very small (maximum $|\Delta V| = 6.9 \times 10^{-5}$ p.u.), and angle differences remain below 0.04° . This indicates that the custom Jacobian implementation and mismatch formulation are numerically consistent with established NR practice [1], [2].

Convergence behavior follows expected algorithm characteristics [5], [3]:

- NR and FDLF converged quickly (3–4 iterations),
- GS converged but required many more updates (18 iterations),
- NR reached the strongest mismatch reduction per iteration.

The residual differences come mainly from:

- printed rounding in PSSE bus report values (4 decimal place display),
- solver stop criteria and internal scaling differences,
- floating-point linear-solve details between implementations.

These observations agree with standard load-flow references and practical tool behavior in commercial packages [3], [6].

III. TASK 3: VOLTAGE SENSITIVITY ANALYSIS

A. Method

Each load bus (5, 6, 8) was perturbed independently by scaling both active and reactive demand with:

$$\alpha \in \{-10\%, 0\%, +10\%\},$$

while all other loads were kept fixed. For each case, the full NR solver was run and all bus-voltage magnitudes were recorded.

For each target load bus, voltage spread was quantified using:

$$\text{Var}(V_b) = \frac{1}{N} \sum_{m=1}^N (V_{b,m} - \bar{V}_b)^2, \quad (5)$$

$$\sigma(V_b) = \sqrt{\text{Var}(V_b)}. \quad (6)$$

To rank overall influence:

$$\text{RMS_STD}_k = \sqrt{\frac{1}{n_b} \sum_{b=1}^{n_b} \sigma_b^2}.$$

B. Voltage Results Under Each Load Variation

TABLE XII: Voltage magnitudes for target load bus 5 variation.

$\Delta P, \Delta Q$	V_1	V_2	V_3	V_4	V_5	V_6	V_7	V_8	V_9
-10%	1.040000	1.025000	1.025000	1.027784	1.001712	1.014125	1.027257	1.017024	1.032976
0%	1.040000	1.025000	1.025000	1.025788	0.995631	1.012654	1.025769	1.015883	1.032353
+10%	1.040000	1.025000	1.025000	1.023640	0.989300	1.011062	1.024214	1.014681	1.031688

TABLE XIII: Voltage magnitudes for target load bus 6 variation.

$\Delta P, \Delta Q$	V_1	V_2	V_3	V_4	V_5	V_6	V_7	V_8	V_9
-10%	1.040000	1.025000	1.025000	1.026885	0.996397	1.016802	1.026146	1.016519	1.033273
0%	1.040000	1.025000	1.025000	1.025788	0.995631	1.012654	1.025769	1.015883	1.032353
+10%	1.040000	1.025000	1.025000	1.024618	0.994804	1.008384	1.025370	1.015219	1.031402

TABLE XIV: Voltage magnitudes for target load bus 8 variation.

$\Delta P, \Delta Q$	V_1	V_2	V_3	V_4	V_5	V_6	V_7	V_8	V_9
-10%	1.040000	1.025000	1.025000	1.025382	0.995196	1.012385	1.026947	1.019141	1.033334
0%	1.040000	1.025000	1.025000	1.025788	0.995631	1.012654	1.025769	1.015883	1.032353
+10%	1.040000	1.025000	1.025000	1.026100	0.995931	1.012799	1.024507	1.012510	1.031298

C. Variance and Standard Deviation Tables

TABLE XV: Variance and standard deviation across buses for target load bus 5.

Observed Bus	Variance	Std Dev
1	0.0000000000	0.0000000000
2	0.0000000000	0.0000000000
3	0.0000000000	0.0000000000
4	0.0000028635	0.0016921912
5	0.0000256833	0.0050678664
6	0.0000015649	0.0012509498
7	0.0000015438	0.0012424893
8	0.0000009147	0.0009564155
9	0.0000002765	0.0005257919

TABLE XVI: Variance and standard deviation across buses for target load bus 6.

Observed Bus	Variance	Std Dev
1	0.0000000000	0.0000000000
2	0.0000000000	0.0000000000
3	0.0000000000	0.0000000000
4	0.0000008571	0.0009257769
5	0.0000004233	0.0006506190
6	0.0000118106	0.0034366545
7	0.0000001004	0.0003169338
8	0.0000002819	0.0005308973
9	0.0000005836	0.0007639111

TABLE XVII: Variance and standard deviation across buses for target load bus 8.

Observed Bus	Variance	Std Dev
1	0.0000000000	0.0000000000
2	0.0000000000	0.0000000000
3	0.0000000000	0.0000000000
4	0.0000000863	0.0002937266
5	0.0000000911	0.0003017733
6	0.0000000295	0.0001718018
7	0.00000009928	0.0009963793
8	0.00000073304	0.0027074721
9	0.0000006908	0.0008311667

TABLE XVIII: Sensitivity ranking using aggregate voltage-spread indices.

Target Load Bus	Mean Std Dev	Max Std Dev	RMS Std Dev
5	0.001193	0.005068	0.001910
6	0.000736	0.003437	0.001250
8	0.000589	0.002707	0.001012

D. Task 3 Figures

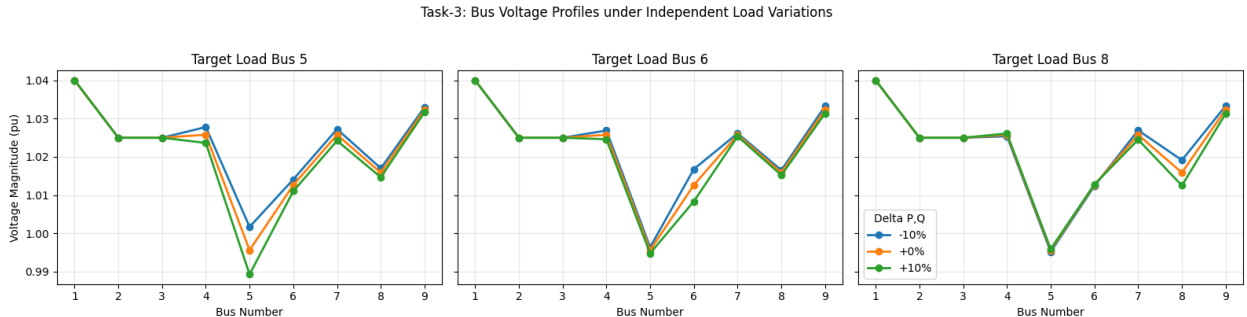


Fig. 8: Voltage profile variation across buses for each target load perturbation.

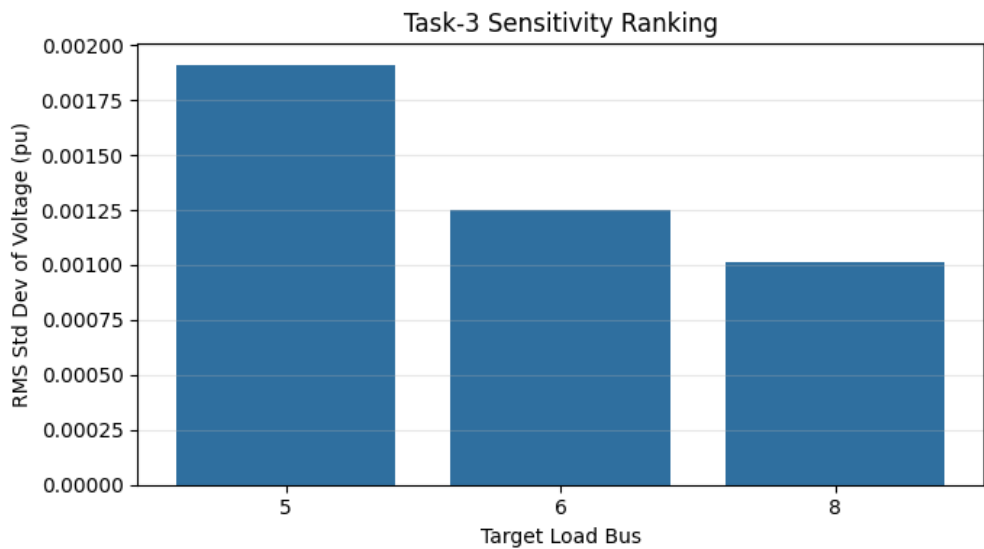


Fig. 9: Sensitivity ranking based on RMS standard deviation.

E. Discussion of Findings

The sensitivity ranking in Table XVIII shows a clear order: bus 5 has the highest network-wide voltage influence, followed by bus 6, then bus 8. This ordering is physically reasonable for the given IEEE 9-bus topology and loading pattern. Bus 5 is connected to bus 4 and bus 7 paths that carry significant active and reactive transfers, so perturbing this load causes larger redistribution of currents and voltage drops in multiple corridors.

The variation tables indicate that generator buses 1–3 remain fixed at their voltage setpoints for all perturbations, which matches PV/slack bus modeling. Most sensitivity appears on PQ buses, especially near the disturbed load bus and along electrically close paths. For the bus-5 perturbation case, V_5 has the largest spread ($\sigma = 0.005068$), while nearby buses 4, 6, and 7 also show notable changes.

For the bus-6 perturbation case, the largest spread occurs at V_6 , and the propagated effect on buses 4, 5, 8, and 9 is moderate. For the bus-8 perturbation case, V_8 dominates the spread, but the global RMS impact is still smaller than the bus-5 case. This confirms that sensitivity is not

only a function of local load size; it also depends on electrical coupling and reactive support paths.

From a planning viewpoint, these results suggest that bus 5 is the most critical candidate for voltage-support actions under demand uncertainty (e.g., local reactive compensation, dynamic VAR support, or tighter operational monitoring). In contrast, bus-8 variations are relatively better contained and less disruptive to the whole system.

The trend is aligned with common load-flow interpretation in standard references: voltage sensitivity rises with stronger network coupling and weaker local reactive margin [3], [7], [4]. Therefore, for operational studies on this system, load uncertainty at bus 5 should receive priority in contingency screening and voltage-security assessment.

Overall, Task 3 confirms that the developed NR solver can be reused for systematic parametric studies, not only for a single base-case solution. The same computational core used in Task 1 produced stable convergence for all 9 sensitivity cases, which supports the consistency and robustness of the implementation.

REFERENCES

- [1] W. H. Tinney and C. E. Hart, "Power flow solution by newton's method," *IEEE Transactions on Power Apparatus and Systems*, vol. PAS-86, no. 11, pp. 1449–1460, 1967.
- [2] J. J. Grainger and W. D. S. Jr., *Power System Analysis*. McGraw-Hill, 1994.
- [3] H. Saadat, *Power System Analysis*, 2nd ed. McGraw-Hill, 1999.
- [4] S. J. Chapman, *Electric Machinery Fundamentals*, 5th ed. McGraw-Hill, 2011.
- [5] B. Stott and O. Alsac, "Fast decoupled load flow," *IEEE Transactions on Power Apparatus and Systems*, vol. PAS-93, no. 3, pp. 859–869, 1974.
- [6] Siemens PTI, "PSS(R)E power system simulator for engineering documentation," <https://www.siemens.com/psse>, 2026, accessed: 2026-02-15.
- [7] A. R. Bergen and V. Vittal, *Power Systems Analysis*, 2nd ed. Prentice Hall, 2000.